Pergamon

Mechanics Research Communications, Vol. 21, No. 6, pp. 645-654, 1994

0093-6413/94 $6.00 + .00

0093-6413(94)00028-X

# FLOW OF NON-NEWTONIAN PARTICULATE SUSPENSION WITH A COMPRESSIBLE PARTICLE PHASE

Ali J. Chamkha, Department of Mechanical Engineering, Kuwait University, Safat, 13060 Kuwait

**Abstract.** Continuum equations for a two-phase fluid-particle flow are developed and applied to the problem of steady, laminar flow over an infinite porous flat plate. Both phases are assumed to behave as non-Newtonian power-law fluids. The effects of particle-particle interaction and diffusion of particles are taken into account in the mathematical model. In addition, the particle phase is assumed to have a non-uniform density distribution. The resulting governing equations are nondimensionalized and solved numerically subject to appropriate boundary conditions using an iterative, implicit finite-difference method. Graphical results for the displacement thicknesses and the skin-friction coefficients for both the fluid and particle phases are presented and discussed to elucidate interesting features of the solutions.

*(Received 30 March 1994; accepted for print 23 April 1994)*

## Introduction

The problem considered in the present paper is that of laminar flow of a two-phase fluid/particle suspension exhibiting non-Newtonian behavior past an infinite porous flat plate with suction being imposed at the surface. This is an ideal problem in which the governing equations reduce to ordinary differential equations and the solution exhibits a boundary-layer type behavior. Most continuum two-phase studies assume that the suspension is Newtonian in nature although theoretical and experimental evidence have shown the opposite as discussed by Soo [1]. It is of interest to consider the case where both the interstitial fluid and particles are treated as having nonlinear power-law stress-strain rate relationships.

The continuum dusty-gas model (meant to represent particulate suspensions having small particle volume fraction) discussed by Marble [2] is generalized to account for particle-phase stresses, particulate diffusion, and non-Newtonian effects as suggested by Soo [1], Peddieson [3], Ramshaw [4], and Fredrickson [5]. Thus, physical mechanisms of collection such as inertial impaction and Brownian diffusion in non-Newtonian suspensions can be predicted when applied to industrial problems involving such flows. There have been some published related work on this problem. Kapur [6] reported closed-form solutions for a power-law fluid flow past an infinite flat plate with uniform suction. Chamkha and Peddieson [7] gave some approximate analytical and numerical results for the Newtonian version of the present problem. While most

of non-Newtonian fluids are highly thermodependent (i.e. their physical properties depend upon temperature, especially, their consistency index), all physical properties will be assumed constants herein as a first approximation. The particle phase is assumed to consist of non-deformable solids of spherical shape and have non-uniform density distribution.

## Governing Equations

Let the plate be placed along the x-axis corresponding to the plane $y=0$. The flow is assumed steady and laminar. The fluid phase is assumed incompressible and the particle phase is assumed compressible and pressureless. At the plate surface, the fluid exhibits uniform suction with a velocity $V_w$.

Taking into account all the assumptions made earlier, the governing equations (which are based on the balance laws of mass and linear momentum for the fluid and the particle phases, see, for instance, Chamkha and Peddieson [7] and Fredrickson [5]) can be summarized as

$$\begin{aligned}
&d_y(\rho_p v_p)=0,\ kd_y((d_y u)^m)+V_w d_y u+(N\rho_p)/\rho(u_p-u)=0,\ d_y P-N(Dd_y\rho_p+\rho_p(v_p+V_w))=0\\
&2^{(n-1)/2}k_p d_y(\rho_p d_y u_p(1/2(d_y u_p)^2+(d_y v_p)^2)^{(n-1)/2})-\rho_p v_p d_y u_p-N\rho_p(u_p-u)=0\\
&2^{(n+1)/2}k_p d_y(\rho_p d_y v_p(1/2(d_y u_p)^2+(d_y v_p)^2)^{(n-1)/2})-\rho_p v_p d_y v_p-N(Dd_y\rho_p+\rho_p(v_p+V_w))=0
\end{aligned} \tag{1}$$

where $\rho$, u, k, and P are the fluid-phase density, velocity in the x direction, phenomenological constant, and pressure, respectively. $\rho_p$, $u_p$, $v_p$, $k_p$ are the particle-phase in-suspension density, velocity in the x direction, velocity in the y direction, and phenomenological constant, respectively. m and n are the fluid and particle behavior coefficient, respectively. N is an interphase force coefficient, and D is a diffusion coefficient. It should be noted that since the particle phase is assumed compressible, the particle phase exhibits a normal velocity gradient which contributes to extra terms in the particle-phase momentum equations. These terms increase the nonlinear coupling between the equations. It is also seen that the hydrodynamic interaction between the phases is restricted to a mutual linear drag force. Other interaction mechanisms such as the virtual force (Zuber [8]), the shear lift force (Saffman [9]), and the spin-lift force (Rubinow and Keller [10]) are neglected compared to the drag force. In the present work N and D will both be treated as constants.

If $k_p$ and D are formally equated to zero, and m and n are equated to unity in Equations (1), the dusty-gas equations discussed by Marble [2] will result. If m and n are replaced by unity and the particle-phase accelerations and stresses neglected in Equations (1), the usual convection Fickian diffusion with body forces will be recovered.

All physical variables will depend on y only because the plate is infinite in length. Equations (1) can be made dimensionless by employing

$$\begin{aligned} &y=(\nu\eta)/V_\infty,\ u=V_\infty F(\eta),\ u_p=V_\infty F_p(\eta),\ v_p=V_\infty G_p(\eta) \\ &P=\rho V_\infty^2 H(\eta),\ \rho_p=\rho_{p\infty} Q_p(\eta),\ \nu=V_\infty^{2(1-1/m)}(k)^{1/m} \end{aligned} \tag{2}$$

where $V_\infty$ and $\rho_{p\infty}$ are the respective free-stream velocity and particle density. It should be noted that when m=1 (Newtonian fluid) then $k=\nu$ (fluid-phase kinematic viscosity), and when n=1 (Newtonian particle phase) then $k_p=\nu_p$ (particle-phase kinematic viscosity). Substituting Equations (2) into Equations (1) and rearranging yield

$$d_\eta(Q_p G_p)=0,\ d_\eta H-\kappa\alpha(\delta d_\eta Q_p+r_v(Q_p-1))=0 \tag{3a,b}$$

$$d_\eta((d_\eta F)^m)+r_v d_\eta F+\kappa\alpha Q_p(F_p-F)=0 \tag{3c}$$

$$2^{(n-1)/2}\beta d_\eta(Q_p d_\eta F_p(1/2(d_\eta F_p)^2+(d_\eta G_p)^2)^{(n-1)/2})-Q_p G_p d_\eta F_p+\alpha Q_p(F-F_p)=0 \tag{3d}$$

$$2^{(n+1)/2}\beta d_\eta(Q_p d_\eta G_p(1/2(d_\eta F_p)^2+(d_\eta G_p)^2)^{(n-1)/2})-Q_p G_p d_\eta G_p-\alpha Q_p(r_v+G_p)-\alpha\delta d_\eta Q_p=0 \tag{3e}$$

where $r_v=V_w/V_\infty$, $\kappa=\rho_{p\infty}/\rho$, $\beta=(k_p V_\infty^{2(n-1)})/\nu^n$, $\alpha=(N\nu)/V_\infty^2$ and $\delta=D/\nu$ are the suction parameter, the particle loading, the viscosity ratio, the inverse Stokes number, and the inverse Schmidt number, respectively.

The boundary conditions employed to solve Equations (3) are

$$F(0)=0,\ F_p(0)=\omega(d_\eta F_p(0))^n,\ H(0)=0,\ G_p(0)=G_{p0}$$
$$\lim_{\eta\to\infty} F(\eta)=1.0,\ \lim_{\eta\to\infty} F_p(\eta)=1.0,\ \lim_{\eta\to\infty} Q_p=0,\ \lim_{\eta\to\infty} G_p=-r_v \tag{4}$$

where $G_{p0}$ and $\omega$ are constants. It is an experimental fact that particles flowing close to a surface experience a certain amount of wall slip. This is taken into account by using the second equation in Equations (4) which is borrowed from rarefied gas dynamics (see, for instance, Soo [11]). In general, $\omega$ will depend on the other parameters of the problem. However, no attempt was made herein to relate $\omega$ to the internal parameters of the suspension.

The displacement thicknesses and the skin-friction coefficients for both the fluid and particle phases are important physical flow properties. These can, respectively, be defined in dimensionless form as

$$\Delta = \int_0^\infty (1-F)\,d\eta,\ \Delta_p = \int_0^\infty (1-F_p)\,d\eta,\ C = (d_\eta F(0))^m,\ C_p = \beta\kappa(d_\eta F_p(0))^n \tag{5}$$

## Results and Discussion

The governing equations for this investigation given earlier are nonlinear and do not exhibit a closed-form solution and, therefore, a numerical solution is desired. An iterative implicit finite-difference scheme similar to that discussed by Blottner [12] and Patankar [13] was used to obtain a numerical solution of Equations (3) subject to Equations (4). Equations (3a) and (3b) were solved for $Q_p$ and H, respectively. Equations (3c-e) were solved for F, $F_p$, and $G_p$, respectively. Equations (3c-e) were discretized using three-point central difference quotients while Equations (3a) and (3b) were discretized using two-point difference quotients and solved

by the trapezoidal rule. Linear tri-diagonal algebraic equations were solved (with iteration being employed to deal with the nonlinear nature of the governing equations) by the Thomas' algorithm as discussed by Carnahan, et al. [14]. Variable step sizes were used and the $\eta$ coordinate was represented by 205 meshes. The initial step size utilized was 0.001 and the growth factor was 1.03. These values were chosen after many numerical tests performed to insure grid independence. When the percent difference between the current and the previous iterations reached 1%, convergence was achieved and the iteration process was terminated. It should be mentioned that due to the highly nonlinear nature of the governing equations, caution must be exercised in obtaining the numerical results. Convergence difficulties were encountered for few cases and were resolved by carefully choosing the initial guesses needed to start the iteration process. A large number of computations were performed and many results were produced. Due to page limitations, only a representative set of graphical results for $G_{p0}$=-2.0 will be presented in figures 1 through 4 to illustrate the effect of the particle behavior coefficient n and the inverse Stokes number $\alpha$ on the solutions.

Figures 1 and 2 depict the changes in the displacement thicknesses $\Delta$ and $\Delta_p$ for both the fluid and particulate phases, respectively as the inverse Stokes number $\alpha$ and the particle-behavior coefficient n change. In these and subsequent figures only the squares have significance. The solid lines simply connect all the squares associated with the same n. As n increases, the domain of viscous effects increases causing $\Delta$ and $\Delta_p$ to increase as shown in figures 1 and 2. At $\alpha$=0, both phases move independently. This is called the frozen condition. However, as $\alpha$ increases, the interaction between the two phases increases causing the velocities parallel to the plate of the fluid and particle phases to increase and decrease, respectively at any

point above the plate. This results in a decrease in the values of $\Delta$ and an increase in the values of $\Delta_p$. These trends are evident from figures 1 and 2. At large values of $\alpha$, equilibrium conditions exist where the relative velocity between the phases is essentially negligible except in the immediate vicinity of the wall because of the differing boundary conditions there.

Figures 3 and 4 present the fluid-phase skin-friction coefficient C and the particle-phase skin-friction coefficient $C_p$ versus $\alpha$ for the same parametric values used in figures 1 and 2. The respective decrease and increase in the values of $\Delta$ and $\Delta_p$ as a result of increasing $\alpha$ mentioned before cause a corresponding increase and decrease in the wall slopes of the velocities parallel to the plate of the fluid and particle phases, respectively. This causes C to increase and $C_p$ to decrease as evident from figures 3 and 4. As the domain of viscous effects increases as a result of increasing n, the slopes of F and $F_p$ at the wall decrease. This yields lower values in C and $C_p$. Verification of the numerical results was made by comparisons with previously published results for Newtonian conditions ($m=1$ and $n=1$) reported by Chamkha and Peddieson [7] and constant particle density non-Newtonian solutions given by Chamkha and Peddieson [15]. While it is desirable to validate the results reported earlier by performing comparisons with experimental data, none was made because such data are lacking at present.

## Conclusion

Numerical solutions for the power-law asymptotic suction profile for a two-phase particulate suspension exhibiting non-uniform particle density distribution are reported. Both phases are assumed to have power-law stress-strain rate relationships. A representative set of graphical results was presented and discussed to show special features of the solutions. It was

found that as the particle behavior coefficient increased from pseudo-plastic type behavior ($n < 1$) to dilatant type behavior ($n > 1$), the displacement thicknesses for both phases increased and the skin-friction coefficients decreased. Also, as the flow transitted from frozen conditions ($\alpha = 0$) to equilibrium conditions at large values of the inverse Stokes number, the fluid-phase displacement thickness decreased while the particle-phase displacement thickness increased. This caused a corresponding increase and decrease in the fluid and particle skin-friction coefficients, respectively. Excellent agreement between the numerical results reported herein and published Newtonian results was achieved.

## References

[1] S. L. Soo, Multiphase Fluid Dynamics, Science Press, (1990).

[2] F. E. Marble, Dynamics of Dusty Gases, Annual Review of Fluid Mechanics, **2** (1970), 397-446.

[3] J. Peddieson, On Continuum Description of Solid-Fluid Suspensions, Developments in Theoretical and Applied Mechanics, **7** (1974), 355-368.

[4] J. D. Ramshaw, Brownian Motion in a Flowing Fluid, Physics of Fluids, **22** (1979), 1595-1601.

[5] A. G. Fredrickson, Principles and Applications of Rheology, Prentice Hall, Inc., (1964).

[6] J. N. Kapur, Flows of Power-Law Fluids Past a Flat Plate with Uniform Suction and Between Two Parallel Plates with Uniform Suction and Injection, Journal of the Physical Society of Japan, **18** (1963), 578-582.

[7] A. J. Chamkha, and J. Peddieson, The Asymptotic Suction Profile For a Particulate Suspension, Developments in Theoretical and Applied Mechanics, **15** (1990), 43-50.

[8] N. Zuber, On the Dispersed Two-Phase Flow in a Laminar Flow Region, Chemical Engineering Sciences, **19** (1964), 897-917.

[9] P. G. Saffman, The Lift Force on a Small Sphere in a Slow Shear Flow, Journal of Fluid

Mechanics, **22** (1965), 385-400.

[10] S. I. Rubinow, and J. B. Keller, The Transverse Force on a spinning Sphere Moving in a Viscous Fluid, Journal of Fluid Mechanics, **11** (1961), 447-459.

[11] S. L. Soo, Pipe Flow of Suspensions, Applied Scientific Research, **21** (1969), 68-84.

[12] F. G. Blottner, Finite Difference Methods of Solutions of the Boundary-Layer Equations, AIAA Journal, **8** (1970), 193-205.

[13] S. V. Patankar, Numerical Heat Transfer and Fluid Flow, McGraw-Hill New York (1980).

[14] B. Carnhan, et al., Applied Numerical Methods, Chapter 7, (1969).

[15] A. J. Chamkha, and J. Peddieson, The Asymptotic Suction Profile For a Power-Law Dusty Gas, Proceedings of the Tenth Canadian Symposium on Fluid Dynamics, **1** (1992), 32-33.

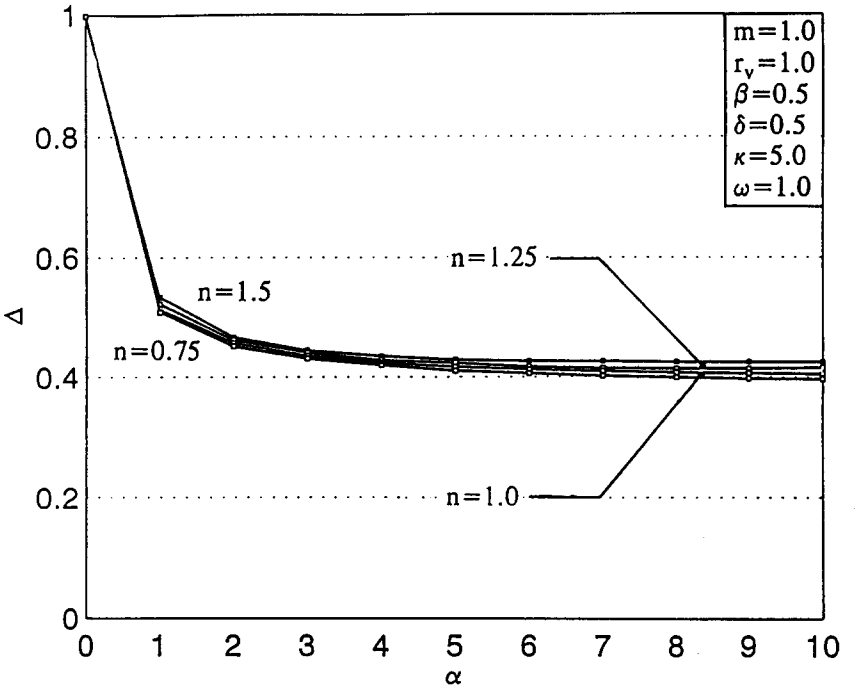


Figure 1. Fluid-Phase Displacement Thickness vs. $\alpha$

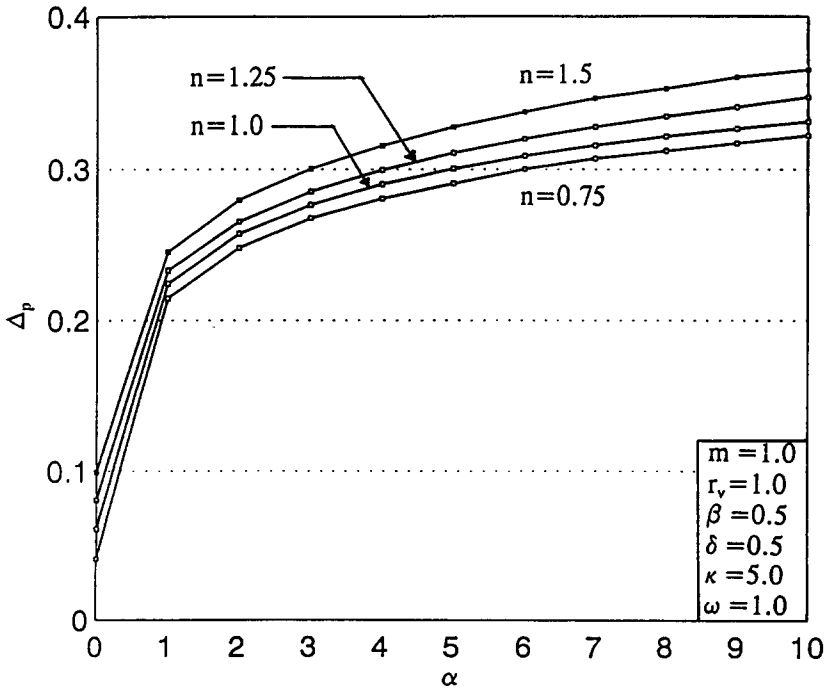


Figure 2. Particle-Phase Displacement Thickness vs. $\alpha$

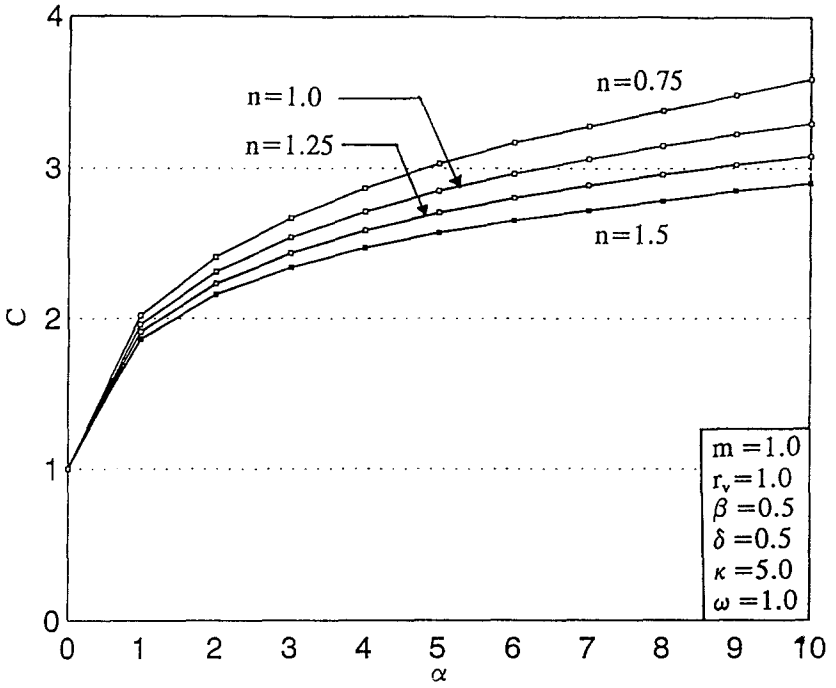


Figure 3. Fluid-Phase Skin-Friction Coefficient vs. $\alpha$

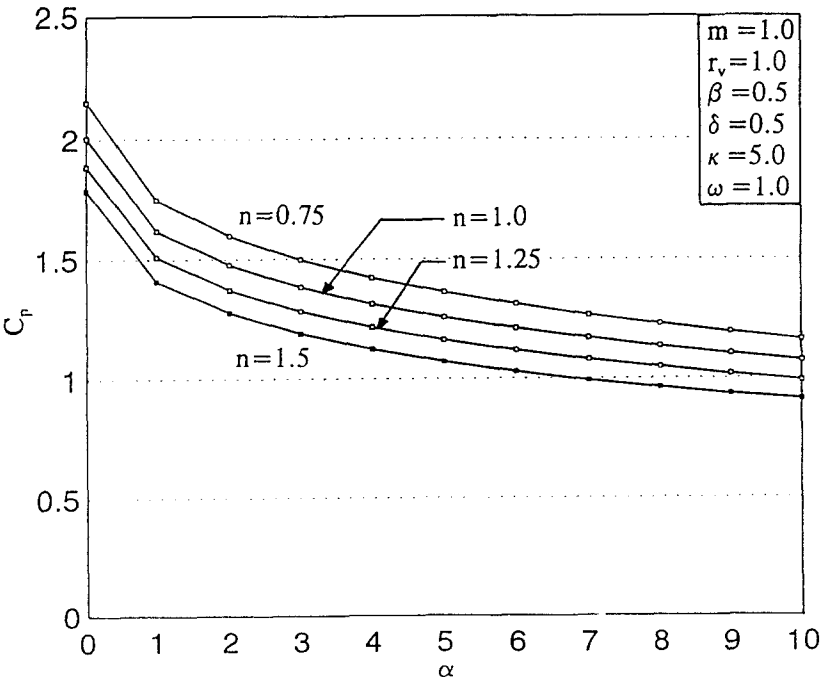


Figure 4. Particle-Phase Skin-Friction Coefficient vs. $\alpha$